Original Article

Chitosan nanoparticles Mitigate Sodium Nitrite Neurotoxicity of Memory and Autophagy Disorders through modulation of immunohistochemical Expression of Neurocan, Beclin-1, and LC3-II

Nada M. Khattab[1], Rania A. Ahmed[1], Sahar K. Darwish[2], and Hani S. Hafez[1]

[1]*Department of Zoology, Faculty of Science, Suez University, Suez, Egypt*

[2]*Department of Histopathology, National Organization for Drug Control and Research (NODCAR), Giza, Egypt*

ABSTRACT

Aim of the Work: The present study aimed to investigate the toxicity of sodium nitrate on memory and learning disorders, brain pathology, and autophagy activity; in addition to the chitosan nanoparticles treatment impacts.

Results: The cognitive activity of novel locations and objects in place and fear of aggravated behavior with the ability to avoid unpleasant stimuli among young rats are negatively influenced by sodium nitrite injection (80 mg/kg) without effects on their ability for new object recognition. Additionally, the toxicity triggered highly distributed degenerated cells with acrocentric chromatin distribution and pyknosis in the CA3 hippocampus sub-region, with a significant increase in the extracellular deposits of beta amyloids and significant up-regulation of neurocan protein. In parallel, there was a defect in the autophagy process through down-regulation of both Beclin 1 and LC3-II expression in the hippocampus CA3 sub-region and dentate gyrus (DG). Meanwhile, chitosan NP improved not only cognitive learning and memory skills for location cognition behavior and the ability to avoid heat shock, but also histopathological structure with decreased distributed degenerated cells and autophagy protein expression modulation with a significant decrease for toxic amyloids.

Conclusion: Our results suggest that CA3 may be considered an important site for controlling the cognitive location novelty and experience of novelty for objects in novel places, but not for detecting the novel objects, in parallel with amelioration of the pathological aspects and inhibition of toxic beta-amyloid deposits. So, chitosan nanoparticles emerged with new insights into their pharmacological activity in the modulation of behavioral disorders and amputation of toxic amyloid aggregation.

Received: 07 June 2022, **Accepted:** 16 July 2022

Key Words: Autophagy, beta amyloids, chitosan nanoparticles, neurotoxicity, sodium nitrite.

Corresponding Author: Hani S. Hafez, PhD, Department of Zoology, Faculty of Science, Suez University, Suez, Egypt, **Tel.**: +20 11 5414 9052, **E-mail:** hani.hafez@suezuniv.edu.eg

ISSN: 1110-0559, Vol. 48, No. 2

INTRODUCTION

Sodium nitrite (NaNO2, E250) is- considered one of the widespread food preservative additives with multifunctional purposes that are used during storage and transportation to prevent detrimental aspects in foods acting as an antimicrobial agent[1-4]. Despite its wide range of use, it has toxic implications due to the potential predisposition of highly carcinogenic nitroso compounds (nitrosamines)[5].

Sodium nitrite has influential oxidizing activities through oxygen transport restriction mechanisms and the formation of methemoglobin[6]. leading to increased inflammatory cytokines production and increased reactive oxygen species (ROS) and destruction of lipid membranes and DNA damage[7-9]. Additionally, due to the brain's high rate of oxidative metabolic activities and high energy demands, it was considered highly susceptible to oxidative injury and subsequent neurodegenerative diseases[10,11]. Moreover, neurocan is a proteoglycan prominently expressed in brain and inhibit neuronal adhesion and neuronal growth in *vitro*[12,13] and may act as a barrier to axonal growth and brain disorders[14,15] during development.

Alzheimer's disease is one of the most well-known neurodegenerative diseases that are thought to be caused by oxidative stress and neuronal function and anatomical impairment with cognitive deficits, aberrant toxic beta-amyloid deposits, neuronal death, and inflammation[13-15]. Specifically, the hippocampus as part of the limbic system has a crucial role in the learning and memory processing mechanism, precisely Cornu ammonis 1 (CA1)[16,17].

Additionally, the cellular autophagy process is crucial in cell survival and functions under normal conditions and enhances the omission process for degraded tissues through the autophagy system to provide a turnover of the nutrients for the cell and specifically neuronal cells[18]. So, its dysfunctional mechanisms may play a precarious role in triggering most neurodegenerative diseases[19]. Precisely, beclin-1 and LC3-II proteins are considered fundamental

DOI: 10.21608/ejh.2022.143405.1700

signals for assessing autophagy mechanisms levels and play a crucial role in its regulation. Beclin-1 stimulates the formation of autophagosomal membranes and LC3-II is thought to be the most reliable marker of active autophagosomes formation[20]. Moreover, beclin1 activity their role in the suppression of mRNA levels of caspase 3 and toxic proteins that invigorated among AD patients' brains and may lead to autophagy impairment[21].

The efforts were dedicated for applying organic extracts with pharmacological activity such as chitosan nanoparticles that have been considered worth drug transporters with biomedical actions due to their biocompatibility and biodegradability[22-24] and brain disorders[25,26].

Additionally, chitosan nanoparticle-based therapies have emerged new insights for neurodegenerative diseases due to their activity for crossing the blood–brain barrier. Jha *et al*[27] revealed that the chitosan-based nanoparticles, bare chitosan, and chitosan copolymerized with PLGA have remarkable activity to inhibit the Aβ1–42 peptide aggregation in *vitro* with inhibition of the formation of β-sheet structure.

Therefore, The purpose of this study was to investigate: 1) The behavioral disorders in learning and memory due to the sodium nitrites injection among young male rats; 2) The histopathological changes and the immunohistochemical expressional level of neurocan in the CA3 sub-region of the hippocampus due to sodium nitrite; 3) The effect of sodium nitrite injection on the expressional levels of autophagy proteins beclin-1 and LC3-II in the CA3 and DG sub-regions; 4) The restorative role of chitosan nanoparticles treatment on the cognitive behavior of learning and memory, the pathology of CA3 of the hippocampus, and the autophagy process disorders due to sodium nitrite injection.

MATERIALS AND METHODS

Chemicals

Chitosan nanoparticles preparation

Briefly, ionotropic gelation of cationic CS polyelectrolyte with sodium tripolyphosphate (STPP) as a crosslinking agent was used to make chitosan nanoparticles (CSNPs). The gelation process was mediated by electrostatic interaction between the quaternized amine groups of CS and the negatively charged counterion (TPP).

Animals

Forty male young albino rats (Sprague-Dawley) weighing about 100-120 g and aged between 8–10 wks, have been included in the current study and obtained from the animal house of the National Research Center, Giza, Egypt. The ARRIVE protocols 2.0 were applied during dealing with the animals. 2.0: The research ethics committee, Approval NO (22412), accepted all methods and updated the criteria for reporting animal research[28]. Extraordinary efforts were taken to keep animal pain, suffering, and discomfort to a minimum, as well as the number of rats included in each experiment. Animals were housed in stainless steel cages and left for two weeks for acclimatization before starting the behavioral experiments. All animals were kept under standardized laboratory conditions (25 OC, 55±5% humidity, and a 12 h light/dark cycle). After 2 weeks of acclimation. The animals were divided into groups as follows: 1) the control group (10 rats) as negative control; 2) the chitosan nanoparticles group injected subcutaneously with 150 mg/kg twice per week for one month (10 rats); 3) 20 rats intraperitoneally injected with NaNo2 (S. nitrite 80 mg/kg)[7], twice per week for one month, later they have been divided into two groups 10 per each; one group was subjected to the behavioral tests considered as a positive group, and the other group was treated subcutaneously with chitosan nanoparticles daily with 150 mg/kg (our lab pilot study) for two weeks and subjected to behavioral tests within the same conditions.

Behavioral Testing

Habituation

All animals were accustomed to the open arena field for two days before the training and tests day, experiments began between 08:30 and10:00 am. Habituation has been carried out with four rats together in the arena for six minutes to roam freely without items. Objects were used and positioned opposite each other at 10 cm from the open field's walls; later rats were taken along individually to the testing room and located in the center of the arena[29]. The floor of the open field (OF) was wiped with a moist towel after each step, and the items were wiped with 70% ethanol[29].

Spontaneous novel object recognition test (What novel object task)

Each rat was evaluated for two random recognition experiments on the third day, with 24-hour pauses between training and testing. A trial phase (3 minutes) and a test phase made up the object recognition test (3 min). Two identical items were positioned diagonally in the open field (OF) arena throughout the trial phase, and the rat was allowed to explore the area. The two objects in the test phase were put in the same position as in the trial phase, with one object being similar to the one in the trial phase (familiar object) and the other being a novel object as shown in (Figure 1a). During the test phase, the locations of items were counter-balanced amongst animals. The following was the formula for novelty preference and discrimination.

(visits to novel – visits to familial)/total visits) * 100 %

The object-location recognition (OLR) test for detection of the Where novelty

The OLR was done in almost the same arena as the object recognition with two different shapes, the trial and the test phases were employed using the sample phase (familiar item-place) and the other was moved to a different location (novel object-place) as shown in (Figure 1b)[30].

Object in place (OiP) for what-where associative memory

The experiment was executed in two phases separated by 30 minutes intervals. The items were presented with four distinct objects (A, B, C, and D) at the corners of the arena, 15 cm from the walls, during the trial phase. Each subject was put in the arena's middle and given 3 minutes to investigate the objects. During the test phase, two of the items (A and C, both on the arena's left) swapped locations, and the participants were given three minutes to examine the objects (Figure 1c). The amount of time spent examining the two things that had moved was compared to the amount of time spent exploring the two objects that had not moved[29,31]. The discrimination ratio was determined as the difference in time spent by each animal investigating item(s) that changed position compared to object(s) that remained in the same position divided by the total time spent exploring all objects in the object-in-place and object location tasks.

Passive avoidance

A shuttle box was used to assess passive avoidance associative learning and memory behavior. This device comprises a sliding door that separates light and a dark room of identical size (20x20x30 cm). The floor of both compartments was constructed from stainless steel bars. On the dark chamber's floor, an isolated stimulator was used to deliver electrical shocks. The trough-shaped equipment had a white lighted section and a dark compartment, which were divided by a downward-opening door. The light section was 12 cm x 11 cm in diameter, while the dark compartment was 25 cm x 11 cm in diameter (in length and height) as shown in (Figure 1D).

Rats were located individually in the light room on the acquisition day (training) and permitted to discover by the door opening and given a 0.5 mA shock for a maximum of 5 seconds by the dark compartment entrance. Later, the animals return to the lightroom with the door reopening. The time rat took to enter the dark chamber was recorded. During the training session, rats that remained for 10s in the light compartment for more than 120s did not enter the dark compartment after the sliding door elevation and did not receive a shock were considered disqualified for the retention test.

To assess long-term memory, a retention test was conducted 24 hours after the acquisition trial concluded. The acquisition trial followed the same pattern as the experiment. The memory retention test was repeated the next day without any shock; the rats were again placed in the illuminated compartment, and the time it took them to visit the dark section was recorded as the retention latency with a maximum retention delay of 180 seconds[32].

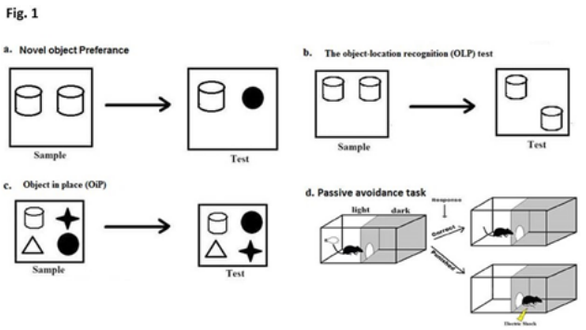

Fig. 1: Diagram of the three object recognition memory tasks. (a) Novel object preference task. (b) Object location task. (c) Object-in-place task. (d) The passive avoidance test.

Methods

Histological examination of the hippocampus complex

Histological and Histochemical Examination

An intraperitoneal dose of 80 mg/kg sodium pentobarbital was used to anesthetize the animals and normal saline and 4% paraformaldehyde in 0.1 M phosphate buffer (PB; pH 7.4) for transcardial perfusion. Brains were collected and cut into two halves; one half was subjected to fixation with 10% neutral buffered formalin and processed for paraffin blocks preparation and cut of coronal section of 5 µm thickness with a rotatory microtome. The other half was fixed in 4% paraformaldehyde (PFA) for 24 h and stored in 30% sucrose for 48 h for immunofluorescence staining using cryostat for 20 µm thickness coronal sections production. Paraffin sections were mounted and subjected to deparaffinization in xylene and descending alcohol series starting from absolute 90%, 70%, 50%, until 30%. The staining used a specific stain and DPX mounting medium.

The following stains were applied:

1. Hematoxylin and Eosin according to the protocol of Bancroft and Gamble[33].
2. The Bielschowsky Silver Stain for neurons structure.
3. The Bielschowsky Stain is an excellent tool for identifying neuron twisting and clumping in the brain. Tissue slices were deparaffinized and hydrated, then submerged in a 20% silver nitrate solution and capped for 20 minutes at 37°C in the dark followed by rinsing in distilled water and then 15 mins immersion in a silver ammonia solution the sections were fixed with 5% sodium thiosulfate for 2 minutes. Finally, the parts were dehydrated, cleaned, and repaired after being rinsed with tap water[34].
4. Histochemical demonstration of Beta amyloids by Congo red stain

Congo red staining was used to detect the beta amyloids plaques using rehydration with graded ethanol and xylene for the deparaffinized coronal sections in xylene. Sections were hydrated and then moved to 50% alcohol for 30 seconds and incubated in 50% ethanol and 0.01% sodium hydroxide in 50 ml for 5 minutes, followed by 20 minutes in a 0.5 percent CR solution. Afterward, slices were incubated in 50% ethanol for 1 minute and 70% ethanol for 1 minute, washed twice with fresh 95 percent ethanol for 2 minutes each rinse, then incubated in 100% ethanol twice for 2 minutes each rinse. Finally, slides were washed twice in xylene for 3 minutes each time before being covered with DPX[12].

4. Immunohistochemical Demonstration of Neurocan Reactivity in CA3 sub-region.

Sections were mounted on positive charge glass slides and treated with 0.3% H_2O_2 in phosphate-buffered saline (PBS) for 30 minutes before being treated with 10% goat serum in phosphate-buffered saline solution with 0.1% Tween™ 20 (PBST) for 30 minutes. The brain tissue slices were cleaned with xylene and subsequently rehydrated with a subtractive series of alcohol after paraffin removal during a 30-minute (60-degree) incubation period. In addition, 10% H_2O_2 was mixed with methanol for a 10-minute treatment to protect against endogenous peroxidase activity. The tris-buffer solution was used to rinse the portion. The antigen retrieve was carried out using citrate buffer for 8 mins. Coronal brain sections were incubated overnight with primary antibody neurocan, C-terminal epitope was employed (dilution ratio, 1:5, Developmental Studies Hybridoma Bank (DSHB)) followed by incubation with rabbit polyclonal secondary antibody in the room for two hours, DAB (obtained from Sigma, USA) was used and hematoxylin was used as counterstaining for microscopic estimation and immunoreactivity estimation[35].

5. Confocal Immunofluorescence Analysis for Beclin-1 and LC3-II Expression in CA3 and dentate gyrus

Immunofluorescence analysis for Beclin-1 and LC3B was performed in frozen tissue sections using rabbit anti-active Beclin-1 (1:100, NB500-249) and rabbit anti-LC3B (1:100 NB100-2220). Secondary antibodies were used for both as follows: goat Anti-rabbit IgG (Alexa Fluor® 488, ab150077) for LC3-II and Goat Anti-rabbit IgG (Alexa Fluor® 647, ab150115) for beclin 1. The fluorescent dye 4–6-diamidino-2-phenylindole-dihydrochloride (DAPI, 1:500, NBP2-31156) was used to stain the sections for 1 h to reveal the nucleus. The sections were observed under a confocal fluorescence microscope (SP8 LIGHTNING confocal microscope) and representative areas were recorded with a digital camera. Image-Pro Plus software was applicated to count positive cells and the total cell number respectively. The average value of the number of the LC3-II positive and Beclin-1-positive neurons was considered as the quantitative value per section[36].

Statistical analyses and Image Analysis

The animal's nose was directed toward the item at a distance of 2 cm was deemed as exploratory activity. Animals that did not complete a minimum of 15 seconds of exploration in the sample phase or 10 seconds of exploration in the test phase were eliminated from the study. Individual variations in the total quantity of exploration were taken into consideration when calculating discrimination between the objects[37,38]. One-way ANOVA and post hoc Newman–Keuls tests were used to compare among groups and a within-groups t-test (two-tailed) and a Pearson correlation coefficient were employed to evaluate if individual groups had discriminated between the items[38,39].

Digital images obtained from CA3 and DG were examined and quantification was performed using the Image J software and processed in Prism 7 software (GraphPad, San Diego, CA, United States), all data have been presented as mean±SE standard errors of the mean for each protein distribution in the CA3 and DG sub-region of the hippocampus of the rat's brain.

RESULTS

Chitosan nanoparticles electron microscopy results

The scanning electron microscope (SEM) and transmission electron microscope (TEM) were used to examine the size and morphology of the chitosan nanoparticles (CSNPs), as shown in (Figures 2 a,b). The SEM micrograph of the CSNPs sample (Figure 2a) displayed irregular-shaped NPs which are predominantly agglomerated in assemblies of a spongy shape and high density. Meanwhile, it can be seen that the NPs with the size range of 8-79 nm were aggregated in the TEM image of CSNPs (Figure 2b). As represented in the size distribution histograms (Figure 2c), the size of CSNPs was in the range of 10-90 nm. Furthermore, the estimated average size for CSNPs was 36.2 nm (Figure 2d). It should be noted that the mean average size of all nanoparticles assessed by zetasizer was larger than the size observed by TEM. This is mostly since the size chosen by zetasizer is a hydrodynamic size in which the NPs are suspended in solutions, which promotes NPs aggregation.

Behavioral results

Novel object recognition (NOR)

Novel object recognition (NOR) behavior was carried out to study associative learning and explicit and episodic memory to estimate the ability of animals to discriminate between familiar and novel objects to test their memory retention ability to identify. The time adjusted to the discrimination time was identified as directing the nose or sitting up toward the object with sniffing interacting behavior with the object. The novel object recognition task was considered a sensitive and reliable memory assessment tool that can detect subtle behavioral cognitive impacts of the different pharmacological compounds.

Animal groups did not reveal statistical significant differences among them for their preferential ability to the novel object recognition either due to sodium nitrite or chitosan nanoparticles treatment. The discrimination ratio for the familiar and novel objects was presented in (Figure 3.I a).

Object location and object in place recognition (where)

Both tests are an important form of spatial memory, with different subcomponents that process specific types of information within memory such as remembering objects, remembering positions, and binding these features in memory. The present study results revealed that sodium nitrite significantly affected the discrimination time for the changed object location with an increased spent interval time of the exploration and decreased discrimination ratio for detecting the new location of the same object with $P<0.001$. While the treated rats with chitosan nanoparticles showed amelioration in the exploration time (decreased time interval) with a high discrimination performance ratio of the familiar object in a different location during the training and test phases experiments with $P<0.01$ compared to the sodium nitrite injected rats as shown in (Figure 3.I b). Additionally, sodium nitrite injected rats showed more increased exploration time of the novel objects in different places (OiP) in comparison to the control group during training and test phases experiments with a value of $P<0.001$. In parallel, the chitosan nanoparticles treated animals showed a higher speed time for recognizing the new location of the new item with high discrimination index with $P<0.01$, respectively compared to the sodium nitrite injected rats as shown in (Figure 3.I c).

The passive avoidance test (PA)

The passive avoidance test was conducted to study the long-term memory. The control animal group revealed a long time for the entrance of the dark compartment during the training phase and test phase with a statistical difference of $P<0.001$; while, the sodium nitrite injected animal group displayed a shorter time for the entrance of the darkroom with small significant difference $P<0.05$ in the training phase (Figure 3.IIa). There was highly significant difference between control and NaNo2 group in the test phase in the second day ($P<0.001$) as shown in (Figure 3.II b). The chitosan nanoparticles increased the retention time of the entrance to the dark room with significant difference in the test phase with value of $P<0.001$ (Figure 3.II c).

Histological results

Hematoxylin and eosin-stained sections

Histological examination of H&E stained slides of the control and chitosan nanoparticles groups revealed microscopically typical structure of hippocampus and prominent granular layer that is composed of closely packed granular cells with rounded vesicular nuclei. The polymorphic layer is composed of pyramidal neurons which appeared as large cells with long processes. Blood capillaries were observed in both molecular and polymorphic layers as shown in (Figures 4 a,b). Chitosan nanoparticles treatment did not induce considerable histopathological alterations in comparison to the control group. However, slight cytoplasmic vacuolation was recorded as shown in (Figure 4c).

The sodium nitrite treated rats displayed highly distributed degenerated cells with acrocentric distributed chromatin with pathological pyknotic nuclei, multiple vacuolated oligodendroglia with prominent chromatolysis features. Additionally, CA3 sub-region revealed obvious perineuronal satellite cells referred to degenerated astrocytes with elongated nuclei and clear space indicating to cellular swelling and distributed neurons with eccentric nuclei and pale cytoplasm. Additionally, sodium nitrite injected rats' revealed increased glial filaments and plump astrocyte with enlarged nuclei called a gemistocyte as shown in (Figures 4 d-g). On the other hand, the chitosan nanoparticles treated group showed few numbers of degenerated cells with normal and homogenous cell distribution in the CA3 sub-region in comparison to sodium nitrite treated animals as shown in (Figures 4 h,i).

Bielschowsky silver stain

Treating animals with chitosan np didn't cause any histological alteration in neurons (Figures 5a,5b) Examination of Bielschowsky silver-stained sections of sodium nitrite injected group revealed microscopically distribution of axonal terminal deformation and dendrites fragmentation with argyrophilic axonal spines (Figure 5c). On the other side, chitosan nanoparticles decreased the number of degenerated and fragmented axons with decreased number of axonal spines and distribution of normal axonal microscopic structures with full neuronal axon and neuron cell body with well-structured dendrites. (Figure 5d).

Histochemical Congo red staining

Congo red was used to demonstrate the beta amyloid deposits in tissues. CA3 sections obtained from control rats appeared with pale pyramidal cells and weak salmon-pink color as shown in (Figure 6.I a). Chitosan nanoparticles did not induce amyloid aggregations in CA3 cells and a scanty salmon color was detected (Figure 6.I.b). Sodium nitrite induced significant increase in congophilic amyloid deposits ($P<0.001$) as shown in (Figure 6.I c) in comparison with control group. The amyloid aggregations appeared as dark salmon-pink homogenous extracellular deposits within the CA3 area. Additionally, treatment with chitosan nanoparticles significantly lessened the amount of aggregated amyloids compared with the sodium nitrite treated group ($P<0.01$) as shown in (Figure 6. I,D).

Immunohistochemical Expression of Neurocan in the CA3 sub-regions of hippocampus

The cytoplasmic neurocan immune-expression was examined in the normal, damaged, and treated hippocampal CA3 sub-region (Figure 7.Ic). On one side, both control and chitosan NP treated groups revealed limited immune-

expression of neurocan (with brownish-green) within CA3 sub-region cells (Figures 7.I a,b). Sodium nitrite induced significant up-regulation of neurocan expression in the extracellular matrix of the CA3 sub-region in the hippocampus with $P<0.001$ in comparison to the control group. On the other side, chitosan NP reduced neurocan expression levels significantly downregulated with $P<0.01$ compared to the sodium nitrite group (injured group) (Figures 7.I a,d, 7.II).

Confocal Immunofluorescences expression of Beclin1 and LC3-II in hippocampus (dentate gyrus (DG) and (CA3)

On one side, the sodium nitrite injected rats group showed that Beclin-1 and LC3-II were significantly decreased in CA3 by $P<0.01$ and $P<0.001$, respectively compared to the control group (Figures 8.Ia-d; Fig. 10a). On the other side, chitosan NP treatment showed up-regulation in the expression of both autophagy proteins with $P<0.05$ and $P<0.01$, respectively as shown in (Figures 8.II a-d). These results indicated that sodium nitrite disturbed the autophagy process in the CA3 area of the (Figures 8.III a,b,c,d; 8.IV a,b,c,d). Further, the analysis of the autophagy proteins expression levels in the dentate gyrus (DG) of the hippocampus revealed that both LC3-II and Beclin-1 in the sodium nitrite rats group were significantly decreased by $P<0.001$ compared to the control group (Figs. 9.III a-d; Fig. 10b) and ameliorated with a significant increase in the treatment group with chitosan NP with $P<0.01$ (Figures 9II a-d and IV a-d and 10b). Additionally, the Co-localization coefficient of two studied autophagy proteins that indicate the formation of the autophagosomes in both the dentate gyrus (DG) and CA3 sub-regions of the hippocampus of the sodium nitrite rats group was significantly decreased with $P<0.001$ compared to the control group; whereas, colocalization coefficients were significantly up-regulated after chitosan NP for both proteins in both DG and CA3 by $P< 0.01$ and $P<0.001$, respectively compared to CA3 in sodium nitrite group (Figure 10c).

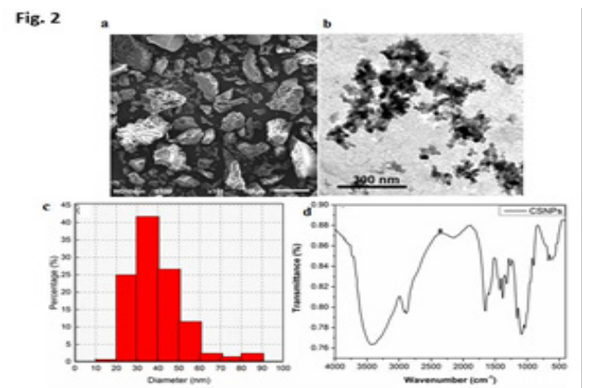

Fig. 2: Photomicrograph of the scanning electron microscope (SEM) and transmission electron microscope (TEM). (a) the SEM micrograph of the CSNPs sample displayed irregular-shaped NPs. (b) TEM image of CSNPs with the size range of 8-79 nm. (c) represented the size distribution histograms, the size of CSNPs was in the range of 10-90 nm.

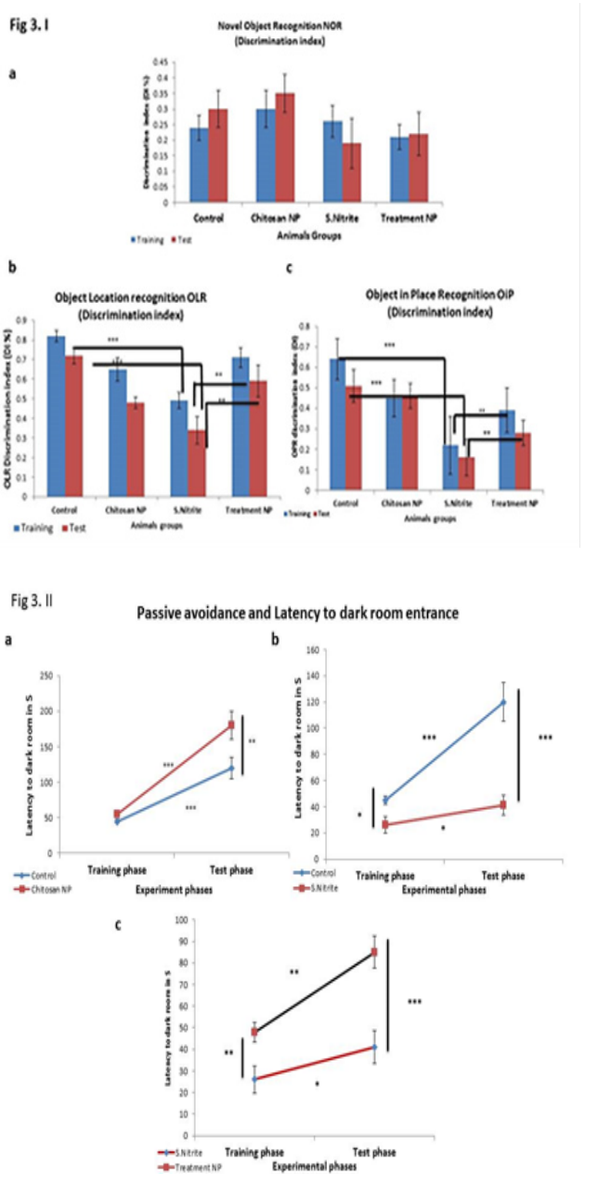

Fig. 3: Graphical representation of performance of the memory behavioral experimental groups of the training and test tasks. (I. a) the novel object preference task; (b) Object location recognition; (c) Object in Place task;(II). the passive avoidance latency time. Experiments were Shown for each group is the mean (SEM) discrimination ratio in the first minute of the test phase only.*$p<0.05$, **$p<0.01$, ***$p<0.001$

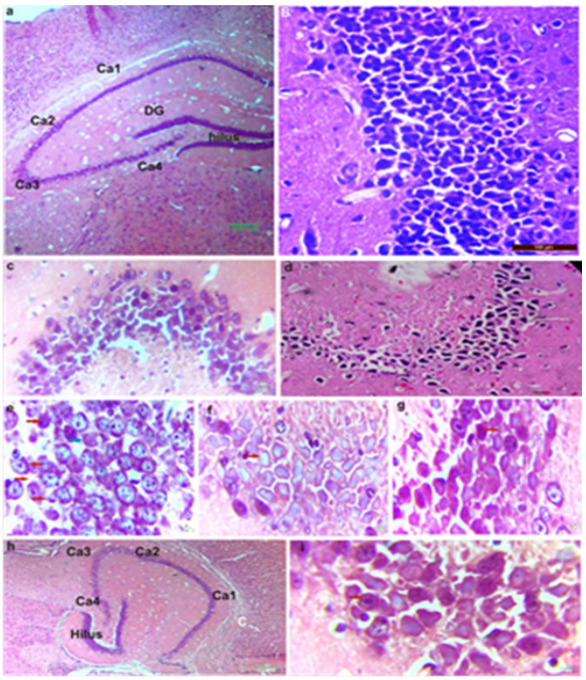

Fig. 4 : Photomicrograph of Hematoxylene and Eosin stained features of the CA3 sub regions of the hippocampus: (a) the control group with normal neuronal structures of the hippocampus.(b) Higher magnification of control section showing CA3 with normal pyramidal cells. (c) CA3 of hippocampus among chitosan nanoparticles injected rats with few vacuolated neurons. (d:g) are hippocampus CA3 sub-region of sodium nitrite treated group reveal the different forms of necrotic and damaged neurons in CA3 sub-region and enlarged nuclei called a gemistocyte (plump astrocyte) (red arrows).(h&i) are photomicrographs of chitosan NP treatment for sodium nitrite injected rats revealed less vacuolated neurons.

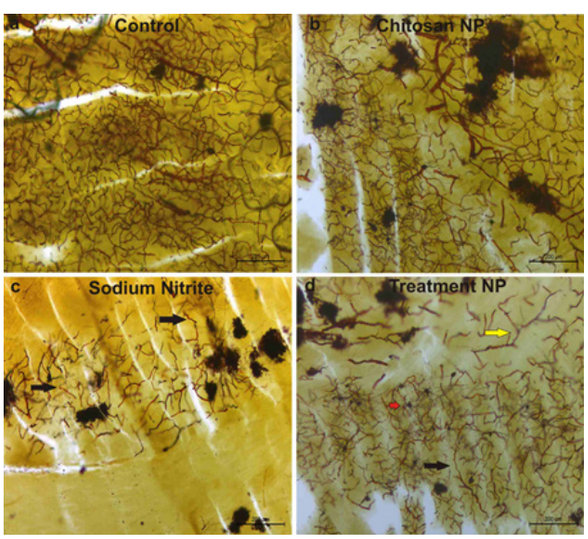

Fig. 5: Photomicrograph of neurons axons stained by Bielschowsky silver nitrite. (a and b), control group and chitosan np, respectively showing normal neuronal soma and dendrites. (c) sodium nitrite injected rats group with axonal terminal and dendrites fragmentation and axonal spines with argyphilic neuron and axons deformation. (d) chitosan NP treated rats group with ameliorated axonal structures.

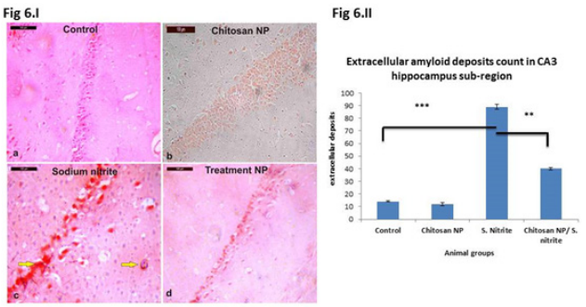

Fig. 6: Photomicrograph of CA3 sub-region stained with Congo red showing congophilic amyloid deposits: I. a. Control group, b. chitosan NP group, c. Increased aggregated beta amyloids in sodium nitrite group. d. Sodium nitrite + chitosan NP treated group showing few congophilic amyloid deposits. II. Graphical representation of the densitometry analysis of amyloid aggregation using Image J. *p<0.05, **p<0.01, ***p<0.001.

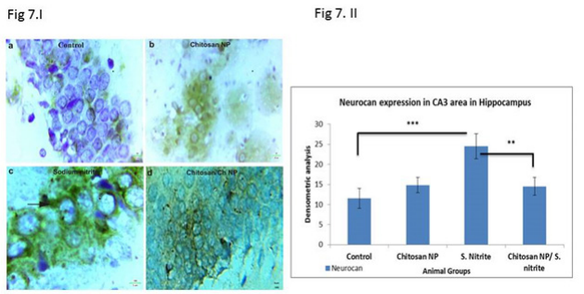

Fig. 7: Photomicrograph of immunoreactivity of anti-neurocan in CA3 area among different groups. (I. a) Negative expression in control group; (I.b) Weak immunoexpression of neurocan in chitosan NP group; (I.c) Strong immunoexpression of neurocan in CA3 cells in sodium nitrite group (black arrow); (I.d) CA3 section obtained from sodium nitrite treated with chitosan NP showing decreased expression of neurocan in CA3 cells compared with sodium nitrite group. II. Graphical representation of the densitometry analysis of neurocan protein expression using Image J. *p<0.05, **p<0.01, ***p<0.001.

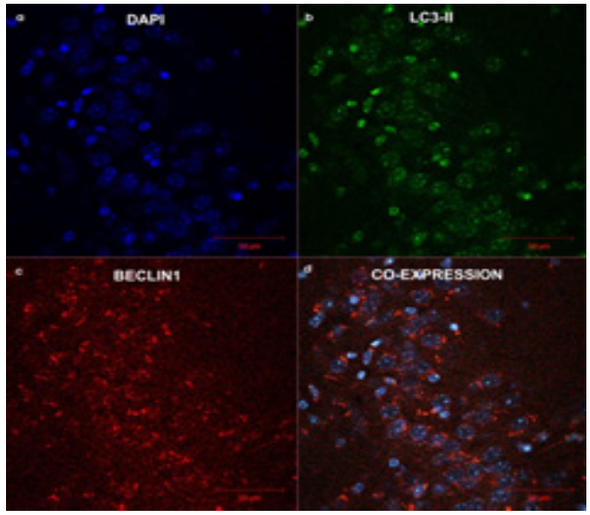

Fig. 8.I: Confocal microscope immunofluorescences analysis for the reactivity with Beclin1 and LC3-II in hippocampal CA3 sub region of control group. (a) DAPI, blue; (b) LC3-II , green; (c) Beclin1, red; (d) Co-localization, mixed colors.

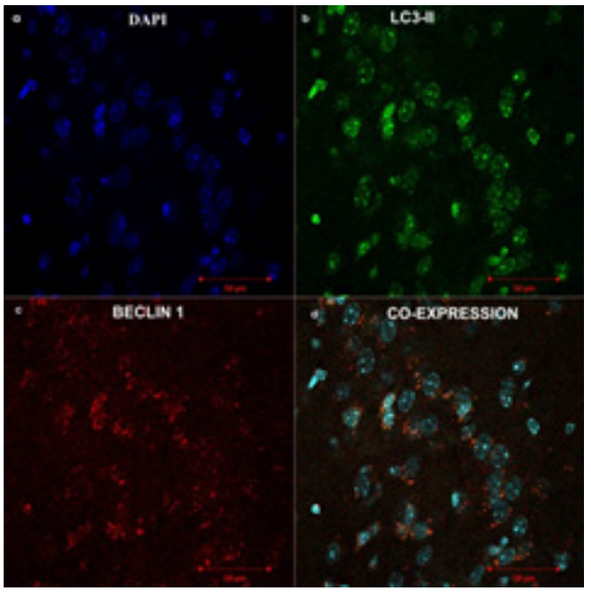

Fig. 8.II: Confocal microscope immunofluorescences analysis for the reactivity with Beclin1 and LC3-II in hippocampal CA3 sub region of chitosan NP treated group. (a) DAPI, blue; (b) LC3-II, green, (c) Beclin1, red; (D) Co-localization, mixed colors.

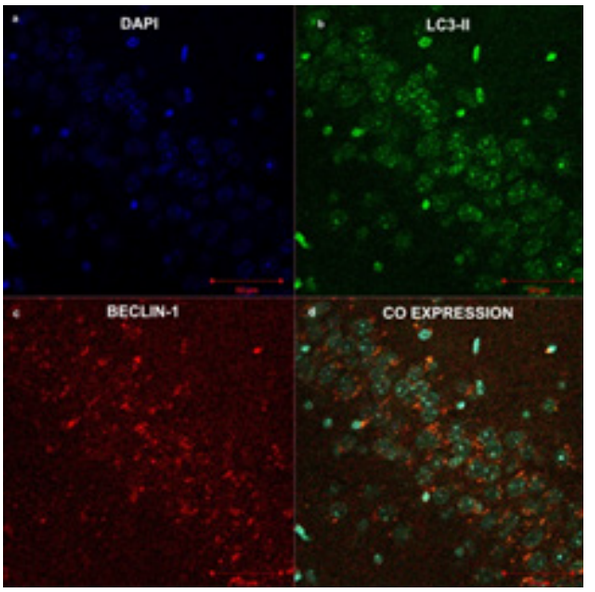

Fig. 8.IV: Confocal microscope immunofluorescences analysis for the reactivity with Beclin1 and LC3-II in hippocampal CA3 sub region of chitosan NP treated group.(a) DAPI, blue;(b), LC3-II, green,(c) Beclin1, red; (D) Co-localization, mixed colors.

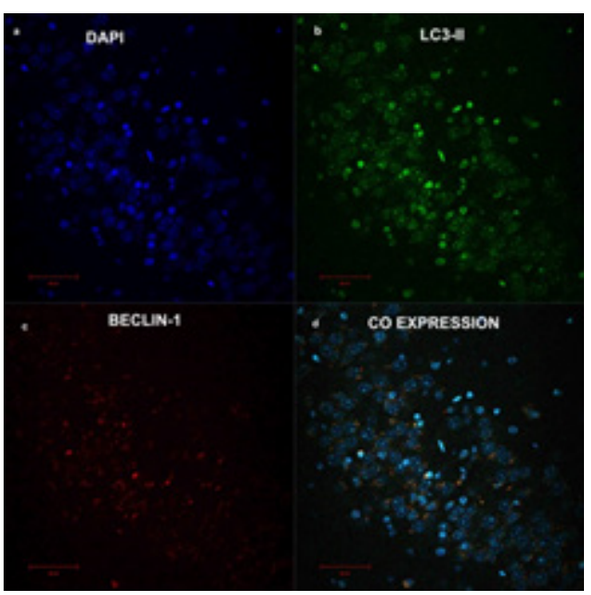

Fig. 8.III: Confocal microscope immunofluorescences analysis for the reactivity with Beclin1 and LC3-II in hippocampal CA3 sub region of chitosan NP treated group.(a) DAPI, blue; (b) LC3-II, green,(c) Beclin1, red; (D)Co-localization, mixed colors.

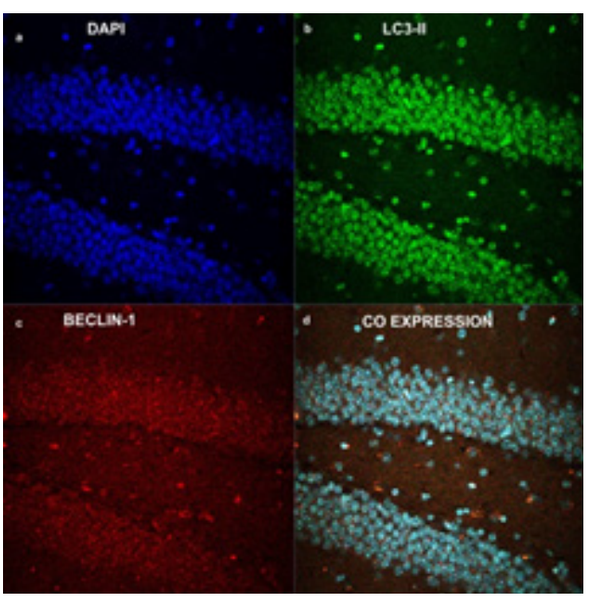

Fig. 9.I: :Confocal microscope immunofluorescences analysis for the reactivity with Beclin1 and LC3-II in hippocampal CA3 sub region of chitosan NP treated group.(a) DAPI, blue(b) LC3-II, green(c), Beclin1, red; (D), Co-localization, mixed colors.

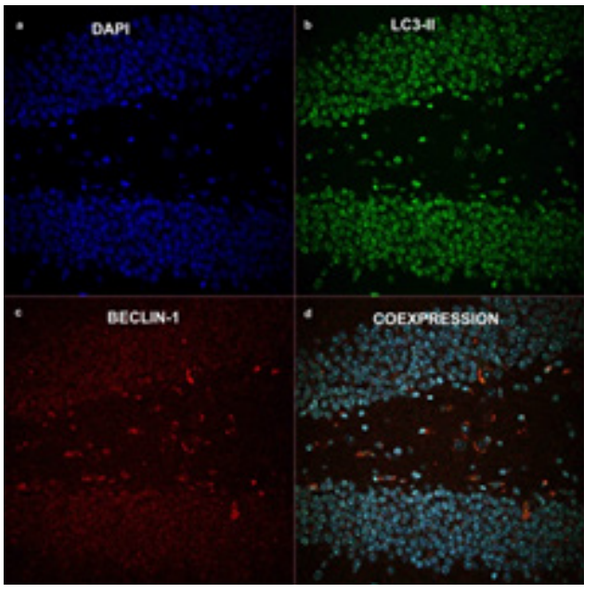

Fig. 9.II: Confocal microscope immunofluorescences analysis for the reactivity with Beclin1 and LC3-II in hippocampal CA3 sub region of chitosan NP treated group.(a) DAPI, blue;(b) LC3-II, green,(c) Beclin1, red(D) Co-localization, mixed colors

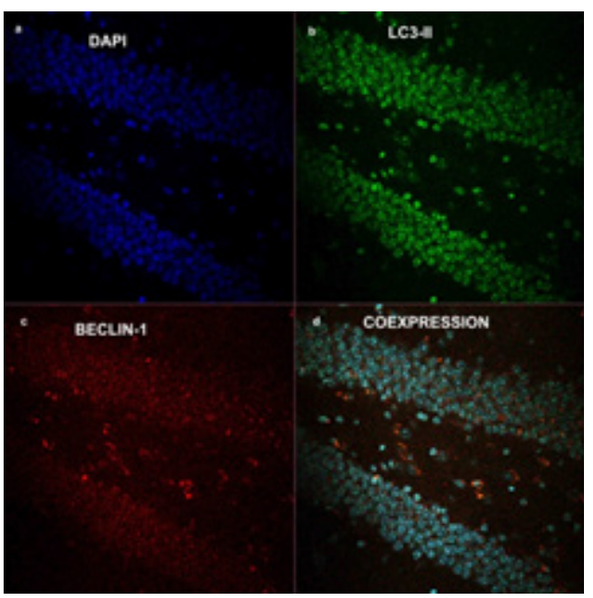

Fig. 9.III: Confocal microscope immunofluorescences analysis for the reactivity with Beclin1 and LC3-II in hippocampal CA3 sub region of chitosan NP treated group(a) DAPI, blue; (b) LC3-II, green,(c) Beclin1, red;(D) Co-localization, mixed colors.

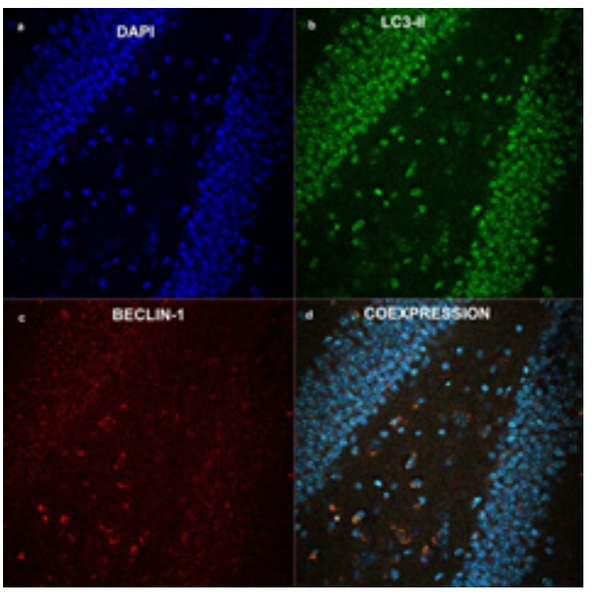

Fig. 9.IV: Confocal microscope immunofluorescences analysis for the reactivity with Beclin1 and LC3-II in hippocampal CA3 sub region of chitosan NP treated group.(a) DAPI, blue;(b) LC3-II, green, (c) Beclin1, red; (D) Co-localization, mixed colors

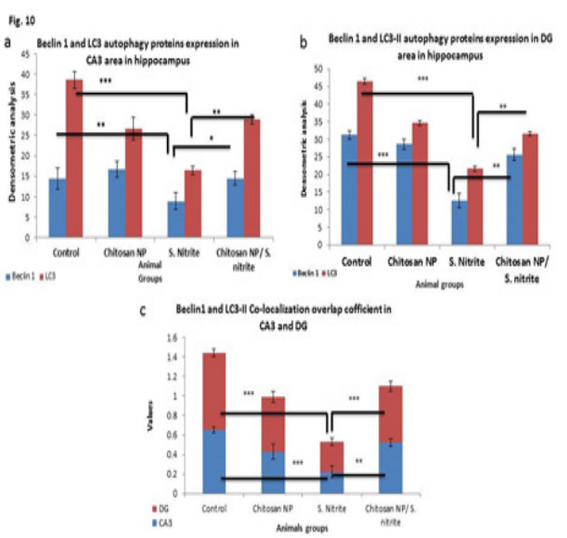

Fig. 10: Graphical representation of the densitometry expression analysis of beclin1 and LC3-II and their co-localization expression overlap coefficient. (a), reveal expression in CA3;(b) Dentate gyrus(c) Their co-localization in both CA3 and DG.

DISCUSSION

Artificial food colors, additives, and other food chemicals are increasingly being utilized among children, resulting in behavioral and developmental impairments as well as learning challenges[40]. Furthermore, early-stage cognitive diseases such as Alzheimer's disease (AD) disclose histological hippocampal deficits frequently report loss of learning/memory capacities as their primary complaint manifestations[41].

Amyloid plaques formation in an AD patient's brain as a result of the production and buildup of Aβ-peptides are considered one of the most serious complications of the disease's development. Plaques eventually developed as a result of the gradual aggregation process from misfolded monomers to soluble protofibrillar aggregates and insoluble fibrils that are the most toxic products for neurons[42].

Therefore, the present study was directed in its main aim to investigate the effective consequent complaints of sodium nitrite supplementation on the young rats learning and memory cognitive behavior activities; and the employment of autophagy pathways for the clearance of toxic beta-amyloid deposits.

The results showed that rats did not reveal significant differences in the animal's ability for recognizing the novel object. The recognition was analyzed through the training and the test phase among all study groups with 24 hour intervals. Further, there were neither discrimination changes with amelioration or deterioration behavior for the novel object among injected rats with NaNO2 nor the treated animals with chitosan nanoparticles. These results may indicate that sodium nitrite does not affect the discrimination ability among rats for detection of the novelty. Furthermore, the novel objects recognition (NOR) is deemed as a reliable and efficient memory evaluation model to identify subtle cognitive and behavioral impairments by measuring working memory and memory consolidation[43]. The non-effective results influencing their behavioral memory performance may be due to injection hassles that triggered negative back draws for their ability of exploration and discrimination time without actual brain damage that may induce real changes in hippocampus discrimination centers. Consequently, Akkerman *et al*.,[44] stated that after a twenty-hour retention interval time, animals may stop items from distinguishing if they had already observed the novel object. Our results were disagree with Fahlström *et al*.,[45] who stated that aged mice faced dysfunction in behavioral memory recognition of new objects and motor disorders. As sodium nitrite injection triggered an effective negative role on young animals' exploration and discrimination ability of the "where" behavior to detect the new place and the new location with increased time for the exploration and low discrimination index among the familiar and novel place for the same object with $P<0.001$ in comparison to control group in both the training and test phases may be due to the effectiveness of sodium nitrite to pass young animals to aged phase. Parallel, there was an ameliorative role for the chitosan NP injection for the consolidation and memory retention activity to detect the new place of the familiar object and new object in a new place with an increased discrimination index.

Furthermore, the multiple pyknotic nuclei and vacuolated oligodendroglia with the prominent chromatolysis of the CA3 hippocampus sub-region due to the sodium nitrite injection may be associated with the consequent behavioral disorders. Altogether, the highly pathological conditions and the up-regulated neurocan expression among sodium nitrite rats groups may clarify the dysfunctional behavior in the recognition of novelty of locations, not objects, and linked to the processing of neural activity of the "where" behavior with CA3 damage. So, the present study may engage the neurocan proteoglycan high expression in CA3 among the NaNO2 injected rats and the level of discrimination for novel places. On contrary, Mandez *et al*.[46] postulated that the CA1 and perirhinal cortex are actively linked to the rate of both objects and place recognition together with c-Fos expression levels affecting real novelty preference, new location, and novel object recognition. Additionally, Zhou *et al*.[47] stated that neurocan expression levels were responsible for the embryological and developmental stages of axonal development functioning as a barrier to axonal growth with a crucial role in axon guidance and neurite formation throughout brain development. The present results demonstrated that neurocan expression is enduring during adulthood with dysfunctional activities due to the sodium nitrite and could be associated with disorders of learning and memory behavior. The revulsive role of neurocan expression was supported by the appearance of the fragmented neuronal axons stained. On the contrary, Dere *et al*.[48] proposed that working memory processing is carried out in the prefrontal cortex area; whereas, memory consolidation in the intact hippocampus functions. Asher *et al*.[49] reported that the distributed glial scars expressing proteoglycans are responsible for brain dysfunction and mainly hinder the regrowth of axons. Moreover, it was plausible to mention that the chitosan NP ameliorated the disordered conditions due to the sodium nitrite injection may be due to the activity of chitosan nanoparticles to induce antioxidant activity that pursues the oxidants and toxic residues produced[22].

Additionally, the current research revealed that sodium nitrite injection has induced significant disturbance for beclin1 and LC3-II expression in both CA3 and DG with various levels of down-regulations, in parallel with significant increase for the beta-amyloid aggregations. While chitosan NP triggered a homeostatic conditional state with modulation of the expression levels and decreased beta amyloids. Therefore, the activity of chitosan nanoparticles may be owned to their ability to anchor to the negatively charged cell surfaces of the deposits and enhancement for their cellular uptake and their activity for adsorption or binding of the peptide on nanoparticles surface[50].

Pickford *et al*.[51] and Spencer *et al*.[52] concluded that beclin-1 levels have dropped in neurodegenerative diseases and impaired autophagy, whereas its up-regulation induced beta-amyloid toxic aggregations reduction with amelioration in the brain functions[53]. Additionally, Hara *et al*.[54] and Komatsu *et al*.[55] correlated the deficiency of Atg5 in the CNS with the dysfunctional progression of neuronal functions parallel with the abnormal aggregated toxic proteins[56,57]. García-Jaramillo *et al*.[58] concluded that sodium nitrite treatment-induced initial loss in learning and memory function. Carvar *et al*[59] claimed that stimulation of proteostasis and autophagy systems are closely linked to the prohibition of uncertain proteins from misfolding or aggregation, or even is sustained in healthy cells by the equilibrium of metabolic mechanisms from protein synthesis to degradation[60,61]. Additionally, LC3 overexpression of microtubule-associated proteins was lipidated into LC3-II triggering the formation of the phagophore with cytoplasmic debris generating complete autophagosome[62]. Moreover, Sachdev *et al*.[63] stated that the autophagy mechanisms upregulated against the nitrosative stress due to their hypoxic impairments impacts in dermal microvascular endothelial cells and pharmacologically targeted inhibitory mechanisms induce autophagy-lysosome actions triggering the degradation of tight junction proteins[64,65]. The apparent modulating activity of the chitosan nanoparticles came through their polycationic nature enhancing their bio-adhesive properties and attachment to cell membranes increasing their penetration properties[66,67]. Santipanichwong *et al*.[68] postulated that electrostatic interactions can cause polysaccharide and protein association, resulting in the production of hybrid polysaccharide-protein particles and increasing nanoparticles penetration and transportation activity specifically in the nervous system[69]. Aktas *et al*.[70] postulated that the chitosan nano-vaccine carrier had favorable permeability of BBB through its activity to associate with FITC (isothiocyano group) beta amyloids lysine amino groups with stable bonding.

CONCLUSION

From the outcome of our investigation, it is possible to conclude that sodium nitrite has negative feedback draws on the young rat's behavioral activities of cognitive recognition activities of novel locations and objects in place but not novel objects. Additionally, sodium nitrite inhibited fear-aggravated behavior test for avoiding aversive stimulus that was used to evaluate learning and memory in rodent models of CNS disorders. Moreover, on one hand, there were impairments in the autophagy mechanisms through the down-regulation of expression of both beclin1 and LC-II with significant beta amyloids Aβ deposits. On the other hand, chitosan NP induced amelioration in the cognitive learning and memory ability concerning the location and place recognition behavior with down-regulation of neurocan in the CA3 sub-region of the hippocampus. So, the findings of our research are quite convincing that CA3 may be more sensitive to the damage than the other hippocampal sub-regions and may be responsible for controlling the novelty of location and object in place cognitive recognition. On the other hand, it was obvious that the nanoparticles were more effective in the modulation of the autophagy proteins in DG than CA3 sub-regions of the hippocampus on cerebellar degeneration in the hippocampus and dentate gyrus through their ability to adsorb onto the toxic aggregations. So, more research into the activity of the sodium nitrite mechanism of distortion on cognitive learning and memory behavior and the ameliorative effects of chitosan nanoparticles is still necessary before obtaining a definitive answer to their role in the up-regulation of autophagy mechanisms.

ACKNOWLEDGMENTS

We have the sincere acknowledgments for the soul of Prof. Abdelrazk Farrag, national research center, Giza, Egypt who facilitated the use of the confocal microscope; Mr. Islam M. Hamza for assisting the researcher with the behavioral tests. And finally, deep thanks to Reda F. Elshaarawy, Professor of Applied Organic Chemistry and materials science, Suez University, Egypt for providing the chitosan nanoparticles.

CONFLICT OF INTERESTS

There are no conflicts of interest.

REFERENCES

1. Gokoglu N. Novel natural food preservatives and applications in seafood preservation: a review. J Sci Food Agric. 2019;99(5):2068–77.
2. Akhzari M, Shafiee SM, Rashno S, Akmali M. Berberine attenuated oxidative stress induced by sodium nitrite in rat liver. Jundishapur J Nat Pharm Prod. 2019;14(1):1–8.
3. Mudan A, Repplinger D, Lebin J, Lewis J, Vohra R, Smollin C. Severe Methemoglobinemia and Death From Intentional Sodium Nitrite Ingestions. J Emerg Med. 2020;59(3):e85–8.
4. Obeid AK, Alsalame HA, Abdulshahed RH. The Role of Moringaoleifrera Seed Extract in Amelioration of Kidney Injury Induced by Sodium Nitrite in Male Rats. Annals of the Romanian Society for Cell Biology. 2021;2392-402.
5. Stoica M, Antohi VM, Alexe P, Ivan AS, Stanciu S, Stoica D, Zlati ML, Stuparu-Cretu M. New Strategies for the Total/Partial Replacement of Conventional Sodium Nitrite in Meat Products: a Review. Food and Bioprocess Technology. 2022;15(3):514–38.
6. Neth MR, Love JS, Horowitz BZ, Shertz MD, Sahni R, Daya MR. Fatal sodium nitrite poisoning: key considerations for prehospital providers. Prehospital Emergency Care. 2021;25(6):844-50.
7. Hassan HA, Hafez HS, Zeghebar FE. Garlic oil as a modulating agent for oxidative stress and neurotoxicity induced by sodium nitrite in male albino rats. Food and chemical Toxicology. 2010;48(7):1980-5.

8. Kuswati K, Handayani ES, Nugraha ZS, Rahmanti FA, Wicaksana ZL, Zhafirrahman M. Propolis inhibited Bax expression and increased neuronal count of hippocampal area CA1 in rats receiving sodium nitrite. Universa Med. 2019;38(2):73.

9. Soliman MM, Aldhahrani A, Elshazly SA, Shukry M, Abouzed TK. Borate Ameliorates Sodium Nitrite-Induced Oxidative Stress Through Regulation of Oxidant/Antioxidant Status: Involvement of the Nrf2/HO-1 and NF-κB Pathways. Biological Trace Element Research. 2022;200(1):197-205.

10. Che H, Li J, Li Y, Ma C, Liu H, Qin J, *et al*. P16 deficiency attenuates intervertebral disc degeneration by adjusting oxidative stress and nucleus pulposus cell cycle. Elife. 2020;9:80–90.

11. Lee KH, Cha M, Lee BH. Crosstalk between Neuron and Glial Cells in Oxidative Injury and Neuroprotection. International Journal of Molecular Sciences. 2021; 22(24):13315.

12. Zhou XH, Brakebusch C, Matthies H, Oohashi T, Hirsch E, Moser M, Krug M, Seidenbecher CI, Boeckers TM, Rauch U, Buettner R, Gundelfinger ED, Fässler R. Neurocan is dispensable for brain development. Mol Cell Biol. 2001; 21(17):5970-8.

13. Vaz M, Silvestre S. Alzheimer's disease: Recent treatment strategies. Eur J Pharmacol. 2020;887:173554.

14. Sarathlal KCS, Kakoty V, Krishna KV, Dubey SK, Chitkara D, Taliyan R. Neuroprotective Efficacy of Co-Encapsulated Rosiglitazone and Vorinostat Nanoparticle on Streptozotocin Induced Mice Model of Alzheimer Disease. ACS Chem Neurosci. 2021;12(9):1528–41.

15. Olayinka JN, Ozolua RI, Akhigbemen AM. Phytochemical screening of aqueous leaf extract of Blighia sapida K.D. Koenig (Sapindaceae) and its analgesic property in mice. J Ethnopharmacol. 2021;273:113977.

16. Tang W, Meng Z, Li N, Liu Y, Li L, Chen D, *et al*. Roles of Gut Microbiota in the Regulation of Hippocampal Plasticity, Inflammation, and Hippocampus-Dependent Behaviors. 2021;10:1.

17. Salahshoor M, Abdolmaleki A, Roshankhah S, Jalali A, Jalili C. Curcumin recovers the toxic effects of nicotine on hippocampus cornu ammonis 1 in rats. Journal of Pharmacology & Pharmacotherapeutics. 2019;10(3):85.

18. Sengking J, Oka C, Wicha P, Yawoot N, Tocharus J, Chaichompoo W, Suksamrarn A, Tocharus C. Neferine protects against brain damage in permanent cerebral ischemic rat associated with autophagy suppression and AMPK/mTOR regulation. Molecular Neurobiology. 2021;58(12):6304-15.

19. Jeong YY, Jia N, Ganesan D, Cai Q. Broad activation of the PRKN pathway triggers synaptic failure by disrupting synaptic mitochondrial supply in early tauopathy. Autophagy. 2022; 19:1-3.

20. Zhao Y, Li ZF, Zhang D, Wang ZY, Wang L. Quercetin alleviates Cadmium-induced autophagy inhibition via TFEB-dependent lysosomal restoration in primary proximal tubular cells. Ecotoxicol Environ Saf. 2021;208:111743.

21. Rana T, Behl T, Sehgal A, Mehta V, Singh S, Bhatia S, *et al*. Exploring the Role of Autophagy Dysfunction in Neurodegenerative Disorders. Mol Neurobiol. 2021;58(10):4886–905.

22. Elbehairi SE, Ismail LA, Alfaifi MY, Elshaarawy RF, Hafez HS. Chitosan nano-vehicles as biocompatible delivering tools for a new Ag (I) curcuminoid-Gboxin analog complex in cancer and inflammation therapy. International Journal of Biological Macromolecules. 2020;165:2750-64..

23. Boominathan T, Sivaramakrishna A. Recent Advances in the Synthesis, Properties, and Applications of Modified Chitosan Derivatives: Challenges and Opportunities. Topics in Current Chemistry. 2021;379(3):1-57.

24. Karavelioglu Z, Cakir-Koc R. Preparation of chitosan nanoparticles as Ginkgo Biloba extract carrier: In *vitro* neuroprotective effect on oxidative stress-induced human neuroblastoma cells (SH-SY5Y). International Journal of Biological Macromolecules. 2021;192:675-83.

25. Xu Y, Asghar S, Yang L, Li H, Wang Z, Ping Q, *et al*. Lactoferrin-coated polysaccharide nanoparticles based on chitosan hydrochloride/hyaluronic acid/PEG for treating brain glioma. Carbohydr Polym. 2017;157:419–28..

26. Cortés H, Alcalá-Alcalá S, Caballero-Florán IH, Bernal-Chávez SA, Ávalos-Fuentes A, González-Torres M, *et al*. A reevaluation of chitosan-decorated nanoparticles to cross the blood-brain barrier. Membranes (Basel). 2020;10(9):1–21.

27. Jha A, Ghormade V, Kolge H, Paknikar KM. Dual effect of chitosan-based nanoparticles on the inhibition of β-amyloid peptide aggregation and disintegration of the preformed fibrils. Journal of Materials Chemistry B. 2019; 7(21), 3362–3373.

28. Percie du Sert N, Hurst V, Ahluwalia A, Alam S, Avey MT, Baker M, Browne WJ, Clark A, Cuthill IC, Dirnagl U, Emerson M. The ARRIVE guidelines 2.0: Updated guidelines for reporting animal research. Journal of Cerebral Blood Flow & Metabolism. 2020;40(9):1769-77.

29. Barker GR, Bird F, Alexander V, Warburton EC. Recognition memory for objects, place, and temporal order: a disconnection analysis of the role of the medial prefrontal cortex and perirhinal cortex. Journal of Neuroscience. 2007;27(11):2948-57.

30. Ishikawa H, Yamada K, Pavlides C, Ichitani Y. Sleep deprivation impairs spontaneous object-place but not novel-object recognition in rats. Neuroscience Letters. 2014;580:114-8.

31. Ameen-Ali KE, Easton A, Eacott MJ. Moving beyond standard procedures to assess spontaneous recognition memory. Neuroscience & Biobehavioral Reviews. 2015;53:37-51.

32. Senechal Y, Kelly PH, Dev KK. Amyloid precursor protein knockout mice show age-dependent deficits in passive avoidance learning. Behavioural brain research. 2008;186(1):126-32.

33. Bancroft, J.D. and Gamble, M. Theory and Practice of Histological Techniques (6th ed.). Churchill Livingstone, Elsevier, 2008.

34. Chen DH, Latimer C, Yagi M, Ndugga-Kabuye MK, Heigham E, Jayadev S, Meabon JS, Gomez CM, Keene CD, Cook DG, Raskind WH. Heterozygous STUB1 missense variants cause ataxia, cognitive decline, and STUB1 mislocalization. Neurology Genetics. 2020;6(2).

35. Edelstein AD, Tsuchida MA, Amodaj N, Pinkard H, Vale RD, Stuurman N. Advanced methods of microscope control using μManager software. Journal of biological methods. 2014;1(2).

36. Xu L, Shen J, Yu L, Sun J, Yan M. Autophagy is involved in sevoflurane-induced developmental neurotoxicity in the developing rat brain. Brain Research Bulletin. 2018;140:226-32.

37. Silvers JM, Harrod SB, Mactutus CF, Booze RM. Automation of the novel object recognition task for use in adolescent rats. J Neurosci Methods. 2007; 15; 166(1):99-103. doi: 10.1016/j.jneumeth.2007.06.032.

38. Cole E, Simundic A, Mossa FP, Mumby DG. Assessing object-recognition memory in rats: Pitfalls of the existent tasks and the advantages of a new test. Learn Behav. 2019; 47, 141–155.

39. Bussey TJ, Duck J, Muir JL, Aggleton JP. Distinct patterns of behavioural impairments resulting from fornix transection or neurotoxic lesions of the perirhinal and postrhinal cortices in the rat. Behavioural brain research. 2000;111(1-2):187-202.

40. Arnold LE, Lofthouse N, Hurt E. Artificial food colors and attention-deficit/hyperactivity symptoms: conclusions to dye for. Neurotherapeutics. 2012 Jul;9(3):599-609. doi: 10.1007/s13311-012-0133-x. PMID: 22864801; PMCID: PMC3441937.

41. Rauk, Arvi (2009). The chemistry of Alzheimer's disease. , 38(9), 2698–0. doi:10.1039/b807980n

42. Jahn H. Memory loss in Alzheimer's disease. Dialogues in clinical neuroscience. 2022;15(4):445–54.

43. Bevins RA, Besheer J. Object recognition in rats and mice: a one-trial non-matching-to-sample learning task to study'recognition memory'. Nature protocols. 2006;1(3):1306-11.

44. Akkerman S, Prickaerts J, Steinbusch HW, Blokland A. Object recognition testing: statistical considerations. Behavioural brain research. 2012;232(2):317-22.

45. Fahlström A, Zeberg H, Ulfhake B. Changes in behaviors of male C57BL/6J mice across adult life span and effects of dietary restriction. Age. 2012;34(6):1435-52.

46. Mendez M, Arias N, Uceda S, Arias JL. c-Fos expression correlates with performance on novel object and novel place recognition tests. Brain research bulletin. 2015;117:16-23.

47. Zhou XH, Brakebusch C, Matthies H, Oohashi T, Hirsch E, Moser M, Krug M, Seidenbecher CI, Boeckers TM, Rauch U, Buettner R. Neurocan is dispensable for brain development. Molecular and Cellular Biology. 2001;21(17):5970-8.

48. Dere E, Huston JP, Silva MA. The pharmacology, neuroanatomy and neurogenetics of one-trial object recognition in rodents. Neuroscience & Biobehavioral Reviews. 2007;31(5):673-704.

49. Asher RA, Morgenstern DA, Fidler PS, Adcock KH, Oohira A, Braistead JE, Levine JM, Margolis RU, Rogers JH, Fawcett JW. Neurocan is upregulated in injured brain and in cytokine-treated astrocytes. Journal of Neuroscience. 2000;20(7):2427-38.

50. Jaruszewski KM, Ramakrishnan S, Poduslo JF and. Kandimalla KK, Nanomedicine, 2012, 8, 250-260

51. Pickford F, Masliah E, Britschgi M, Lucin K, Narasimhan R, Jaeger PA, Small S, Spencer B, Rockenstein E, Levine B, Wyss-Coray T. The autophagy-related protein beclin 1 shows reduced expression in early Alzheimer disease and regulates amyloid β accumulation in mice. The Journal of clinical investigation. 2008;118(6):2190-9.

52. Spencer B, Potkar R, Trejo M, Rockenstein E, Patrick C, Gindi R, Adame A, Wyss-Coray T, Masliah E. Beclin 1 gene transfer activates autophagy and ameliorates the neurodegenerative pathology in α-synuclein models of Parkinson's and Lewy body diseases. Journal of Neuroscience. 2009;29(43):13578-88.

53. Shibata M, Lu T, Furuya T, Degterev A, Mizushima N, Yoshimori T, MacDonald M, Yankner B, Yuan J. Regulation of intracellular accumulation of mutant Huntingtin by Beclin 1. Journal of Biological Chemistry. 2006;281(20):14474-85.

54. Hara T, Nakamura K, Matsui M, Yamamoto A, Nakahara Y, Suzuki-Migishima R, Yokoyama M, Mishima K, Saito I, Okano H, Mizushima N. Suppression of basal autophagy in neural cells causes neurodegenerative disease in mice. Nature. 2006;441(7095):885-9.

55. Komatsu M, Waguri S, Chiba T, Murata S, Iwata JI, Tanida I, Ueno T, Koike M, Uchiyama Y, Kominami E, Tanaka K. Loss of autophagy in the central nervous system causes neurodegeneration in mice. Nature. 2006;441(7095):880-4.

56. Bingol B, Sheng M. Deconstruction for reconstruction: the role of proteolysis in neural plasticity and disease. Neuron. 2011;69(1):22-32.

57. Hernandez D, Torres CA, Setlik W, Cebrián C, Mosharov EV, Tang G, Cheng HC, Kholodilov N, Yarygina O, Burke RE, Gershon M. Regulation of presynaptic neurotransmission by macroautophagy. Neuron. 2012;74(2):277-84.

58. García-Jaramillo M, Beaver LM, Truong L, Axton ER, Keller RM, Prater MC, Magnusson KR, Tanguay RL, Stevens JF, Hord NG. Nitrate and nitrite exposure leads to mild anxiogenic-like behavior and alters brain metabolomic profile in zebrafish. PloS one. 2020 31;15(12):e0240070.

59. JCarver JA, Ecroyd H, Truscott RJ, Thorn DC, Holt C. Proteostasis and the regulation of intra- and extracellular protein aggregation by ATP-independent molecular chaperones: lens α-crystallins and milk caseins. Accounts of Chemical Research. 2018;51(3):745-52.

60. Walczak M, Martens S. Dissecting the role of the Atg12–Atg5-Atg16 complex during autophagosome formation. Autophagy. 2013;9(3):424-5.

61. Lim J, Yue Z. Neuronal aggregates: formation, clearance, and spreading. Developmental cell. 2015;32(4):491-501.

62. Rubinsztein DC, Bento CF, Deretic V. Therapeutic targeting of autophagy in neurodegenerative and infectious diseases. Journal of Experimental Medicine. 2015;212(7):979-90.

63. Sachdev U, Cui X, Hong G, Namkoong S, Karlsson JM, Baty CJ, Tzeng E. High mobility group box 1 promotes endothelial cell angiogenic behavior in *vitro* and improves muscle perfusion in *vivo* in response to ischemic injury. Journal of vascular surgery. 2012;55(1):180-91.

64. Han S, Yu B, Wang Y, Liu Y. Role of plant autophagy in stress response. Protein & cell. 2011;2(10):784-91.

65. Wang Y, Tao TQ, Song DD, Liu XH. Calreticulin ameliorates hypoxia/reoxygenation-induced human microvascular endothelial cell injury by inhibiting autophagy. Shock: Injury, Inflammation, and Sepsis: Laboratory and Clinical Approaches. 2018;49(1):108-16.

66. Lim J, Yue Z. Neuronal aggregates: formation, clearance, and spreading. Developmental cell. 2015;32(4):491-501.

67. Lim C, Hwang DS, Lee DW. Intermolecular interactions of chitosan: Degree of acetylation and molecular weight. Carbohydrate Polymers. 2021;259:117782..

68. Santipanichwong R, Suphantharika M, Weiss J, McClements DJ. Core shell biopolymer nanoparticles produced by electrostatic deposition of beet pectin onto heat denatured β lactoglobulin aggregates. Journal of Food Science. 2008 Aug;73(6):N23-30.

69. Ballabh P, Braun A, Nedergaard M. The blood–brain barrier: an overview: structure, regulation, and clinical implications. Neurobiology of disease. 2004;16(1):1-3.

70. Aktaş Y, Andrieux K, Alonso MJ, Calvo P, Gürsoy RN, Couvreur P, Çapan Y. Preparation and in *vitro* evaluation of chitosan nanoparticles containing a caspase inhibitor. International journal of pharmaceutics. 2005;298(2):378-83.

الملخص العربى

دور جزيئات الشيتوزان النانوية على تخفيف السمية العصبية التي يسببها نتريت الصوديوم لاضطرابات الذاكرة والالتهام الذاتي من خلال تعديل التعبير الكيميائي المناعي Neurocan و Beclin-1 و LC3-II.

ندى خطاب[١]، رانيا أحمد[١]، سحر درويش[٢]، هاني حافظ[١]

[١]قسم علم الحيوان ، كلية العلوم ، جامعة السويس ، السويس ، مصر

[٢]قسم أمراض الهيستوباثولوجيا ، الهيئة القومية للرقابة والبحوث الدوائية ، الجيزة ، مصر

الهدف: تهدف هذه الدراسة إلى التحقيق في سمية نترات الصوديوم على أمراض الدماغ والسلوك الإدراكي للذاكرة ونشاط الالتهام الذاتي مع تحسين ظروف جزيئات الشيتوزان النانوية.

النتائج: يتأثر النشاط المعرفي للمواقع والأشياء الجديدة الموجودة في الفئران الصغيرة إلى حد كبير (P <٠,٠٠١) بامتصاص نتريت الصوديوم (٨٠ مجم / كجم) ، وليس للأشياء الجديدة. علاوة على ذلك ، فإن نتريت الصوديوم يثبط الخوف ويؤدي إلى تفاقم السلوك لتجنب المحفزات غير السارة (P <٠,٠٠١) ، والتي كانت فعالة في تقييم عجز التعلم والذاكرة. أثارت السمية خلايا متدهورة موزعة بشكل كبير مع توزيع كروماتين acrocentric وبنية مرضية حلقية على المنطقة الفرعية CA٣ قرن آمون ، مع زيادة كبيرة في الترسبات داخل الخلايا من بيتا أميلويد (P <٠,٠٠١) والتنظيم التصاعدي الكبير لـ neurocan P <٠,٠٠١. بالتوازي ، كان هناك خلل في عملية الالتهام الذاتي بسبب التنظيم الخافت لكل من تعبير Beclin ١ و II-LC٣ مع P <٠,٠١ و P <٠,٠٠١ ، على التوالي ، وفي التلفيف المسنن مع P <٠,٠٠١ لكلا البروتينين. وفي الوقت نفسه ، عزز الكيتوزان NP ليس فقط التعلم المعرفي ومهارات الذاكرة للسلوك الإدراكي للموقع والقدرة على تجنب الصدمة الحرارية ولكن أيضًا مستوى التشريح المرضي مع تناقص الخلايا المتدهورة الموزعة وتعديل تعبير بروتينات الالتهام الذاتي مع انخفاض كبير في الأميلويد السامة ف <٠,٠١.

الخلاصة: تشير نتائجنا إلى أن CA٣ قد يكون مهمًا للتحكم في حداثة الموقع المعرفي وتجربة الجدة التي لا تكتشف الأشياء الجديدة. لذلك ، ظهر الشيتوزان np كنشاط دوائي في تعديل الاضطرابات السلوكية مع دور البتر ضد تراكم الأميلويد السام.